Journal of Environmental Chemical Engineering 8 (2020) 104549

Contents lists available at ScienceDirect

Journal of Environmental Chemical Engineering

journal homepage: www.elsevier.com/locate/jece

Degradation of anionic azo dyes in aqueous solution using a continuous flow photocatalytic packed-bed reactor: Influence of water matrix and toxicity evaluation

Vincenzo Vaiano [a], Olga Sacco [b,*], Giovanni Libralato [c], Giusy Lofrano [b,d], Antonietta Siciliano [c], Federica Carraturo [c], Marco Guida [c], Maurizio Carotenuto [b]

[a] Department of Industrial Engineering, University of Salerno, via Giovanni Paolo II, 132, 84084 Fisciano, SA, Italy
[b] Department of Chemistry and Biology "A. Zambelli", University of Salerno, via Giovanni Paolo II, 132, 84084 Fisciano, SA, Italy
[c] Department of Biology, University of Naples Federico II, via Cinthia ed. 7, 80126, Naples, Italy
[d] Centro Servizi Metereologici e Tecnologici Avanzati (CeSMA), University of Naples Federico II, Via Cinthia 21, 80126, Naples, Italy

ARTICLE INFO

Editor: G. Palmisano

Keywords:
Continuous flow photocatalytic packed-bed reactor
Anionic azo-dyes
Water matrix
Toxicity

ABSTRACT

A continuous flow photocatalytic packed-bed reactor irradiated by UV-LEDs was employed for the degradation of two toxic anionic azo dyes: Eriochrome Black-T (EBT) and Methyl Orange (MeO). Commercial anatase TiO_2 in pellets form was used as packing material for the photoreactor. The experimental tests were carried out using both distilled and tap water as aqueous matrix for the two selected dyes. The influence of the liquid flow rate on the performances of the photocatalytic packed-bed reactor was investigated in the range 0.5–2.1 mL/min. Photocatalytic results showed that, under UV light, the system allows to achieve steady-state dyes concentration values without deactivation phenomena in 510 min irradiation time. Using distilled water, the highest efficiency of the process (EBT and MeO decolorization of about 100 % and 90 %, respectively) was observed with a liquid flow rate of 0.5 mL/min (contact time =6.6 min). In the presence of tap water and using the same contact time, the EBT decolourization was still total whereas MeO degradation was lower and equal to 70 %. For this reason, the photocatalytic reactor was followed by an adsorption unit based on the use of activated carbon. With such configuration, the complete MeO decolourization was achieved.

The total removal of toxicity for EBT was achieved with just one packed-bed reactor being the toxicity of potential by-products not relevant. In the case of MeO, the full toxicity removal was obtained only after powdered activated carbon filtration.

1. Introduction

In recent years, the fate of a series of chemical pollutants, including contaminants of emerging concern, in the aquatic environment has gained growing interest. Little is still known about the effects of dyes released into water bodies [1–3]. Dyes are extensively used in various industrial sectors including plastic, printing, food, paper, gasoline, pharmaceutical, and textile industries [4]. The global dyes and pigments market is expected to rise up to USD 37,623.08 million by 2023 with an estimated annual growth rate of 5.46 % (2018–2023). Textile segment occupies a major share of the dye market in terms of type, volume, and complexity worldwide [1]. A very large fraction of synthetic dyes used by dyeing industries are composed of azo dyes. Reactive azo dyes are characterized by one or more azo groups (—N═N—) that act as chromophore in the molecular structure [5]. During the dyeing process around 10–15 % of the dye is lost and discharged into the effluents, leading to potential toxic effects to both humans and the environment if not properly removed. Due to their chemical structure and synthetic origins, dyes are resistant to fading on exposure to light, temperature, and many chemicals. The compounds containing the azo group are difficult to degrade even at low concentrations because of their resistance to light, heat, chemicals and microbial action. Therefore, it is very difficult to remove azo dyes by means of conventional wastewater treatments [6–9]. These features, coupled with their toxicity, make azo dyes a possible source of ecological concern, especially for freshwater aquatic ecosystems [2]. The presence of dyes in natural water bodies

* Corresponding author.
E-mail address: osacco@unisa.it (O. Sacco).

https://doi.org/10.1016/j.jece.2020.104549
Received 24 July 2020; Received in revised form 14 September 2020; Accepted 23 September 2020
Available online 30 September 2020

leads to a decline in light diffusion which in turn distresses the photochemical activities of species present in the aquatic streams or structures [2,10]. Their partial degradation by bacteria results in the formation of toxic amines [11,12]. Several studies underlined the toxicity of textile azo dyes [2,13–16], showing potential adverse effects [17]. Despite their continuous release worldwide, the impact of dyes and their residues have been scarcely evaluated since now. With ever-increasing ecological awareness, the environmental legislation and regulatory authorities are now more concerned about the hazardous nature of industrially-related synthetic dyes and dyes-containing hazardous wastewater effluents [1, 18].

Eriochrome Black T (EBT) and Methyl orange (MeO) are considered among the most problematic dyes in wastewater [19]. EBT is a toxic and carcinogen anionic azo dye which is used as an indicator in complexometric titrations and for dyeing nylon, silk and wool fibers [20,21]. Likewise, MeO finds extensive applications in textiles, plastics, cosmetics, dye manufacturing industries [22]. MeO exhibits environmental hazard and toxicity to human health and can cause breathing, diarrhoea, vomiting and nausea [19]. They are both considered as recalcitrant to biological treatments, therefore alternative methods have been recently attempted for their removal from wastewater, mainly adsorption processes [19,20,22]. Several adsorbents such as magnetite/pectin and magnetite/silica/pectin hybrid nanocomposites [23], activated carbon [24], anionic layer double hydroxide [25], $NiFe_2O_4$ magnetic nanoparticles [26], modified ostrich bone waste [22] and epibromohydrin modified crosslinked polyamine resin [19] have been applied for the removal of EBT and MeO from aqueous solutions. Although good results were achieved with these methods, these adsorbents were expensive and difficult to synthesize. Moreover, once exhausted, the material used in the adsorption process must be handled as hazardous waste becoming itself a source of contamination [27]. Various studies related to the regeneration of adsorbents (i.e., thermal, chemical, microbiological and vacuum regeneration) have been carried out to compensate for the disadvantages of the adsorption technique, obtaining a certain degree of success [28]. Nevertheless, these techniques are generally limited either from a technical and economic point of view. More recently advanced oxidation processes [21,29,30] have also been attempted. Heterogeneous photocatalysis based on titanium dioxide has been successfully employed in the decolorization of organic dyes from the textile industry [31]. Generally, the photocatalytic process involves the generation of free radicals that are able to oxidize pollutants several pollutants, such as dyes [32–35]. In particular, the organic dyes adsorbed onto the catalyst surface can be converted into harmless compounds such as carbon dioxide and water. However, the use of TiO_2 in powder form is disadvantages because a separation step is required after the photocatalytic treatment in order to reuse the recovered photocatalyst particles [36–40] and this could be one reason to still limited large-scale applications of a photocatalytic process for the wastewater treatment [41]. Moreover, the wastewater treatment photoreactors filled with a catalyst in macroscopic forms have a unique advantage to avoid filtration step to separate and reuse the catalyst from the treated effluent [42, 43]. Other reasons that prevented the development of this technology is the absence of proper reactor design and optimization because of the most studied photoreactors are in batch configuration [44–47], so it is desirable to evolve a continuous flow reactor since batch treatment systems would be not useful for practical applications. Several research papers were focused on the use of continuous-flow photoreactor with immobilized TiO_2 [48–50] but most papers deal only with the evaluation of the dyes decolourization. At our knowledge, scientific literature about the employment of a continuous-flow reactor for water depollution through the dual evaluation of photocatalytic decolourization and its related toxicity is still limited [41]. The aim of present work is to test a continuous flow photocatalytic packed-bed reactor filled with commercial TiO_2 pellets in order to remove EBT and MeO azo dyes from aqueous solutions and their related toxicity, including biological models belonging to various trophic levels like *R. subcapitata*, *L. sativum* and *D. magna*.

2. Materials and methods

2.1. Materials

The commercial TiO_2 pellets (T_PTs) in cylindrical shape (size: 12.5 mm × 5.5 mm) were provided by Sigma Aldrich. The pelletized activated carbon (PaC) in cylindrical shape, used as adsorption materials, (FILTERCARB KI 60; size: 11 mm × 4 mm; specific surface area (BET): 1000-1100 m^2/g) were provided by Carbonitalia. Eriochrome Black-T ($C_{20}H_{12}N_3O_7SNa$) and Methyl Orange ($C_{14}H_{14}N_3NaO_3S$) anionic azo-dyes were purchased from Sigma Aldrich. Distilled and tap water (Table 1) were used for preparing all the aqueous solutions used in the tests.

2.2. Sample characterization

The N_2 adsorption-desorption isotherm at −196 °C was performed with Sorptometer 1042 instrument (Costech). BET and T-plot methods were used for the specific surface area of T_PTs while Barret–Joyner–Halenda (BJH) method was applied for the determination of pore size distribution. Before the analysis, the sample was pre-treated at 150 °C for 30 min in He flow. UV–vis reflectance spectra (UV–vis DRS) were recorded with a PerkinElmer spectrometer Lambda 35 using a RSA-PE-20 reflectance spectroscopy accessory (Labsphere Inc., North Sutton, NH). Wide-angle X-ray diffraction (XRD) patterns were obtained using a micro-diffractometer Rigaku D-max-RAPID, using Cu-Kα radiation and a cylindrical imaging plate detector. Laser Raman spectra were obtained at room temperature with a Dispersive MicroRaman (Invia, Renishaw), equipped with 514 nm laser, in the range 100–800 cm^{-1} Raman shift.

2.3. Photocatalytic tests using packed-bed reactor operating in batch and continuous mode

The experimental setup consists of a packed-bed photocatalytic micro-reactor, an external stirred aerated tank containing the polluted solution and a peristaltic pump to provide a continuous flow of water along the photocatalytic reactor. The packed-bed reactor is a cylindrical pyrex reactor (ID =1.3 cm, L_{TOT} =10 cm and V_{TOT} =7 mL) filled with 4 g of T_PTs. The packed-bed reactor was irradiated by a UV LEDs strip (provided by *LEDlightinghut*; nominal power: 12 W/m; wavelength emission peak: 365 nm) positioned around and in contact with external surface of the cylindrical body. The photon flux at reactor external body of packed-bed photoreactor was measured using a spectro-radiometer (StellarNet Inc) and it was about 25 $mW \cdot cm^{-2}$. All the photocatalytic tests were performed at the spontaneous pH of the polluted solutions and the temperature of the system was in the range 20−30 °C during all the performed tests. The photocatalytic experiments were conducted both in batch and continuous mode. In the case of batch mode, the total volume of the treated solution was 100 mL and the system was left in dark

Table 1
Physical and chemical characteristics of tap water.

Conductivity	493 μS/cm
pH	7.23
CO_2	10 mg/l
SiO_2	8.2 mg/l
HCO_3^-	326 mg
Ca	85.8 mg
SO_4^{2-}	23.0 mg
Mg	18.5 mg
Cl^-	6.8 mg
Na	4.1 mg
NO_3^-	3 mg
K^+	1.2 mg
F-	<0.2

condition for 2 h before to switch on the UV-LEDs in order to reach adsorption–desorption equilibrium of the pollutant on the T_PTs surface. The total irradiation time was equal to 180 min. The overall liquid stream is fed from the bottom of the reactor and liquid stream passes through the catalytic bed and finally comes out from the top of the reactor, being conveyed in the same tank used for feeding the reactor. The liquid sample was withdrawn from the tank. For the experimental condition in continuous modes, the liquid flow rate was varied in the range 0.5–2.1 mL/min using a peristaltic pump (*Watson Marlowe 120 s*). The aqueous solution containing the pollutant to be removed was prepared and collected in the feed tank (3 L). The feed tank is equipped with a magnetic stirrer to assure the complete homogenization of the stock solution. The overall liquid stream is fed from the bottom of the reactor and liquid stream passes through the catalytic bed and finally comes out from the top of the reactor, being conveyed in a tank where the treated solutions were collected. The liquid sample was withdrawn at the outlet of the continuous flow micro-reactor. The photocatalytic tests were carried out using two anionic azo dyes: Eriochrome Black T (EBT) and Methyl Orange (MeO) at 10 mg/L initial concentration. In both experimental modes, the liquid samples were analyzed by spectrophotometric measurements (Perkin Elmer UV–vis spectrophotometer) in order to determine the concentration of EBT (at $\lambda = 574$ nm) [51] and MeO (at $\lambda = 464$ nm) [52].

2.4. Ecotoxicity and data analysis

Toxicity was investigated in accordance to [53,54] via a battery of toxicity tests including biological models belonging to various trophic levels (*D. magna, R. subcapitata,* and *L. sativum*). Toxicity tests with *D. magna* were carried out according to [55]. Newborn daphnids (< 24 h old) were exposed in four replicates for 24 and 48 h at 20 ± 1 °C under continuous illumination (1000 lx). Before testing, they were fed with *R. subcapitata* (300,000 cells/mlad libitum. All toxicity tests included the assessment of negative and positive controls in accordance with the specific reference method. Toxicity was expressed as percentage of effect. Microalgae growth inhibition test with *R. subcapitata* was carried out according to [56]. Cultures were kept in Erlenmeyer flasks. The initial inoculum contained 10^4 cells/mL. The specific growth inhibition rate was calculated considering 6 replicates exposed at 20 ± 1 °C for 72 h under continuous illumination (6000 lx). Effect data were expressed as percentage of growth inhibition. Phytotoxicity tests were carried out according to [57] on *L. sativum*. The germination index (GI, %) was considered as endpoint [58]. All endpoints were assessed in triplicate including negative (ultrapure water) and positive (H_3BO_3) controls. The GI can assume values greater or lower than 100 %, where a value equal to 100 % means that the seedling average length and germination rate between a specific treatment and the negative control are the same [59]. If values are between 80 % and 120 %, the effects are likely the negative controls, otherwise values greater than 120 % indicate biostimulation and lower than 80 % inhibition effects. Toxicity data were analysed according to [60]. According to [61], the hazard classification system based on percentage of effect (PE) includes a Class I for PE < 20 % (score 0, no acute hazard), Class II for 20 % ≤ PE < 50 % (score 1, slight acute hazard), Class III for 50 % ≤ PE < 100 % (score 2, acute hazard), Class IV when PE = 100 % in at least one test (score 3, high acute hazard) and a Class V when PE = 100 % in all bioassays (score 4, very high acute hazard). Finally, the integrated class weight score was determined by averaging the values corresponding to each microbiotest class normalised to the most sensitive organism (highest score). Data were checked for normality (Shapiro-Wilk (S-W)test) and homogeneity of variance (F-test) prior to the application of parametric methods (one-way analysis of variance, ANOVA) to compare the potential significant differences between treatments and negative controls. If S-W or F-test failed, non-parametric methods were used (Kruskal-Wallis one-way analysis of variance ranks). Post-hoc Tuckey's method was used to check all pairwise multiple comparison procedures (only significant differences were evidenced). The minimum level of acceptable significance was set at $\alpha = 0.05$. Data were processed by means of SigmaPlot version 11.0, from Systat Software, Inc., San Jose California USA, www.systatsoftware.com.

3. Results and discussion

3.1. T_PTs photocatalyst characterization

The T_PTs sample was characterized using different techniques.

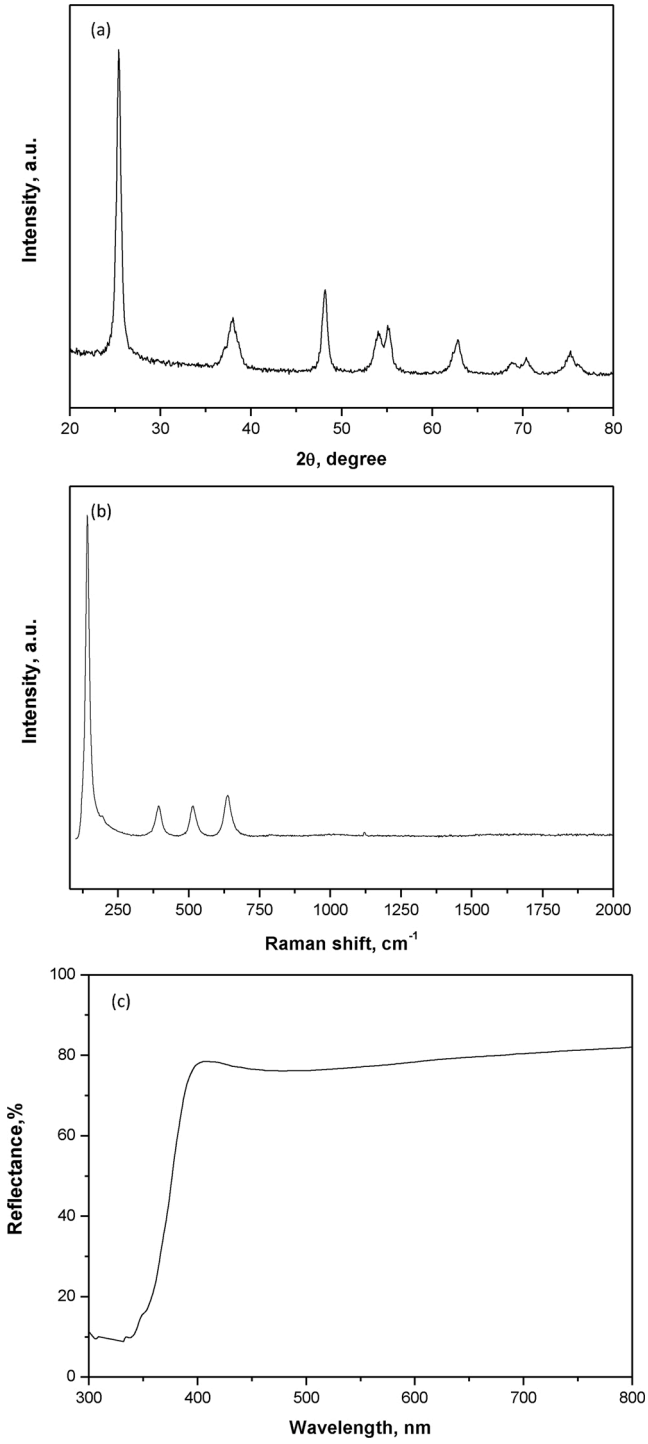

Fig. 1. a) XRD pattern, b) Raman and c) UV–vis reflectance spectrum of T_PTs catalyst.

Fig. 1 reports the XRD diffraction pattern, Raman and UV–vis DRS spectra.

In particular, the crystallinity and the crystal phases of T_PTs sample were examined by XRD analysis (Fig. 1a). Several well-defined diffraction reflections are detectable at 2θ = 25.4°, 38.1°, 48°, 54.1°, 55.2°, 62.7°, 68.9°, 70.5° and 75.2° that are related to TiO_2 crystals in tetragonal anatase phase [62]. The average crystallite size of T_PTs sample calculated for the diffraction plane (1 0 1) (corresponding to the peak at 25.4°) was estimated according to the Scherrer equation and the obtained value is reported in Table 2. The TiO_2 crystallite size was found to be equal to 16 nm, a value very close to commercial PC105 titania in anatase phase [62,63]. In agreement with the XRD data, all Raman active modes (Fig. 1b) positioned at 144, 197, 399, 513, 519 and 639 cm^{-1} are associated to TiO_2 in anatase phase [64,65]. UV–vis DRS spectrum of T_PTs (Fig. 1c) showed that the absorption onset of this sample was around 390 nm, which is typically found for commercial TiO_2 samples in anatase phase [63]. The optical band gap of the T_PTs (Table 2) was determined using the Kubelka-Munk equation. Also in this case, the obtained band gap value (3.2 eV) falls in the range expected for the TiO_2 material in anatase phase [66], meaning that the T_PTs photocatalyst can be activated by the UV light emitted by LEDs used in the photocatalytic tests. The results of N_2 adsorption-desorption measurements at −196 °C are reported in Fig. 2 and Table 2.

The adsorption (Fig. 2a) increased gradually with the relative pressure (p/p_0) due to the adsorption of N_2. As shown in Fig. 2a, the isotherm is identified as type IV, which is typical for mesoporous materials [67]. Moreover, the adsorption-desorption isotherm of T_PTs sample exhibited one hysteresis loops, lying from 0.5 up to 0.9 p/p_0 values. The Barrett-Joyner-Halenda (BJH) pore size distribution is displayed in Fig. 2b. T_PTs exhibits the mean pore size at about 6 nm, evidencing only the presence of mesopores. This result was confirmed by the values of micro- and meso-surface area (Table 2). In fact, the sample showed a value of micro-surface area (10 m^2/g) very lower than meso-surface area (95 m^2/g).

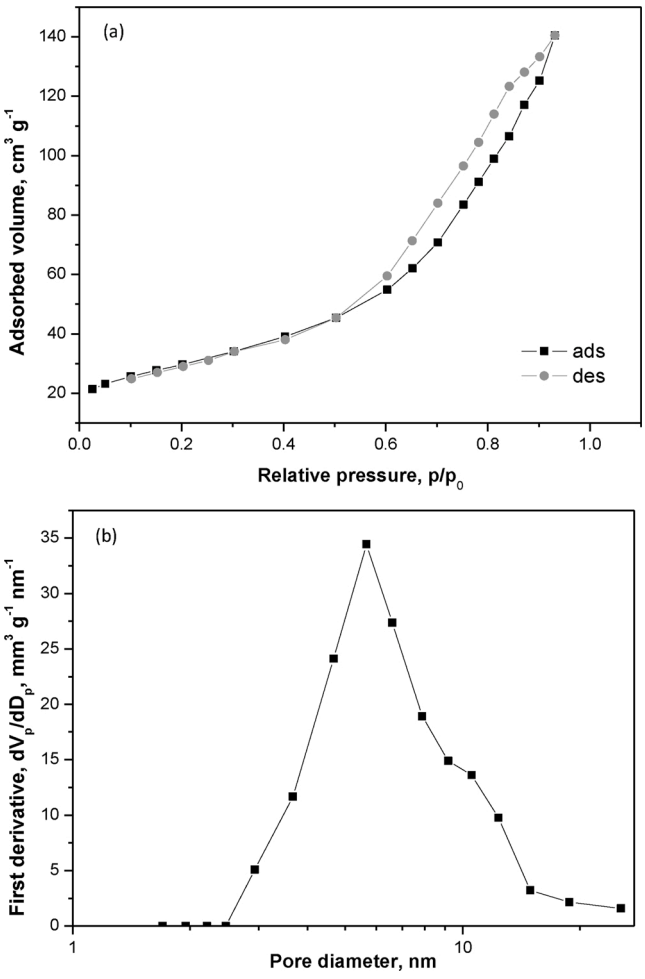

Fig. 2. N_2 adsorption and desorption isotherms (a) and pore size distribution curve (b).

3.2. Photocatalytic tests using the packed-bed reactor operating in batch mode

Preliminary photocatalytic tests were driven using the packed-bed reactor operating in batch mode. The experimental results in terms of EBT and MeO decolourization as a function of irradiation time were reported in Fig. 3.

It is worthwhile to note that, during the photolysis test (carried in the absence of photocatalyst) no EBT [68] or MeO [69] decolourization was observed. On the contrary, the presence of T_PTs photocatalyst led to a significant decrease of EBT and MeO relative concentration, reaching the total EBT and 86 % MeO decolourization after 180 min of UV irradiation. The different trend observed for the decolourization of the two anionic tested dyes could be ascribed to the presence of two sulphonate groups in EBT structure (while there is only one in MeO), inducing to the EBT molecules a more electronegative surface than MeO, thus resulting in more favourable adsorption of EBT on the surface of T_PTs sample [23,70,71]. The previous observation is confirmed from the experimental results obtained after 120 min of run time in dark conditions (data not shown). In fact, EBT decolourization was equal to 93 %, while MeO was not adsorbed by T_PTs. The experimental data strengthen the hypothesis that adsorption and orientation of the dye molecules on the surface of the catalyst could determine the mode of the target dye

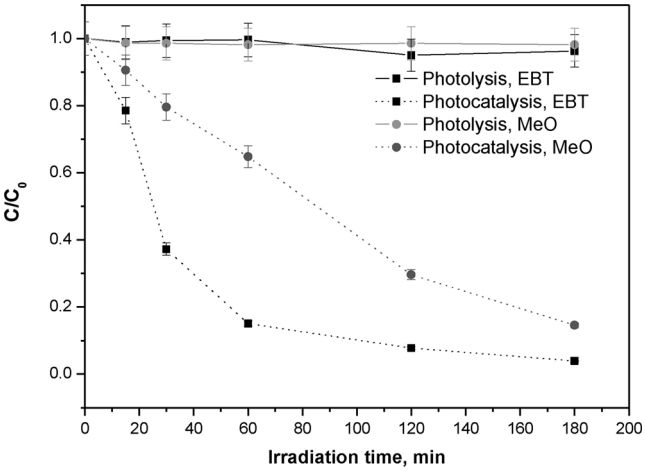

Fig. 3. Photolysis and Photocatalytic EBT and MeO decolourization under UV light using T_PTs catalyst in the packed-bed reactor operating in batch mode; EBT and MeO initial concentration: 10 mg/L; T_PTs catalyst amount: 4 g; Solution volume 100 ml.

Table 2
Chemical physical characterization results of TiO_2 pellets.

Sample	Crystallite size (nm)	Band gap energy (eV)	Surface area (m^2/g)		
			BET	*Micro*	*Meso*
T_PTs	16	3.2	105	10	95

decolourization.

3.3. Photocatalytic tests using the packed-bed reactor operating in continuous mode

For the scale-up of a photocatalytic system for water treatment, a continuous process is desirable to demonstrate a higher flexibility and efficiency compared to a batch system, due to its ability to keep constant the pollutant concentration when the system reaches the steady state condition [72].

3.3.1. Photolysis, adsorption and adsorption /photocatalytic activity tests on T_PTs photocatalyst

Fig. 4 shows the comparison of the photolysis, adsorption test in dark conditions and adsorption/photocatalytic test performed with T_PTs photocatalyst.

From the results reported in Fig. 4a, it is possible to observe that during the photolysis test, the only electromagnetic radiation emitted by the UV LEDs does not provide sufficient energy for the degradation of EBT dye. In fact, also for very long irradiation time, only a very little reduction of concentration was obtained (about 1 %). A different trend was observed for the adsorption test. In the first 3 min of run time, the active sites of T_PTs sample were available to adsorb EBT molecules, reaching a decolourization degree of about 30 %. After 3 min of run time, a gradual increase of EBT concentration was observed until to reach the initial concentration value after about 100 min, indicating the complete saturation of the T_PTs catalytic bed. Fig. 4a reports also the result obtained with the adsorption/photocatalytic test. As it is possible to observe, the presence of UV light induced a decolourization of EBT equal to 45 % after 300 min of test time. This value has remained constant for the entire duration of the adsorption/photocatalytic test and this is attributable to the contribution of the photocatalytic action promote by T_PTs catalytic bed that was to not subjected to deactivation phenomena. The presence of UV light is able to activate the T_PTs sample that can generate hydroxyl radicals able to oxidize the EBT molecules adsorbed on the T_PTs surface, making continuously available the active sites of T_PTs for the adsorption of further EBT molecules [41]. Fig. 4b shows the experimental results observed for the decolourization process of MeO. Both the photolysis test (presence of the only UV radiation) and dark adsorption showed no efficiency in the removal of dye molecules according to the collected data in batch configuration (Fig. 3). On the contrary, the adsorption/ photocatalytic test immediately showed about 20 % of MeO decolourization and this value remains unchanged for the overall duration of the test (510 min). This decrease in MeO concentration is attributable only to the photocatalytic contribution.

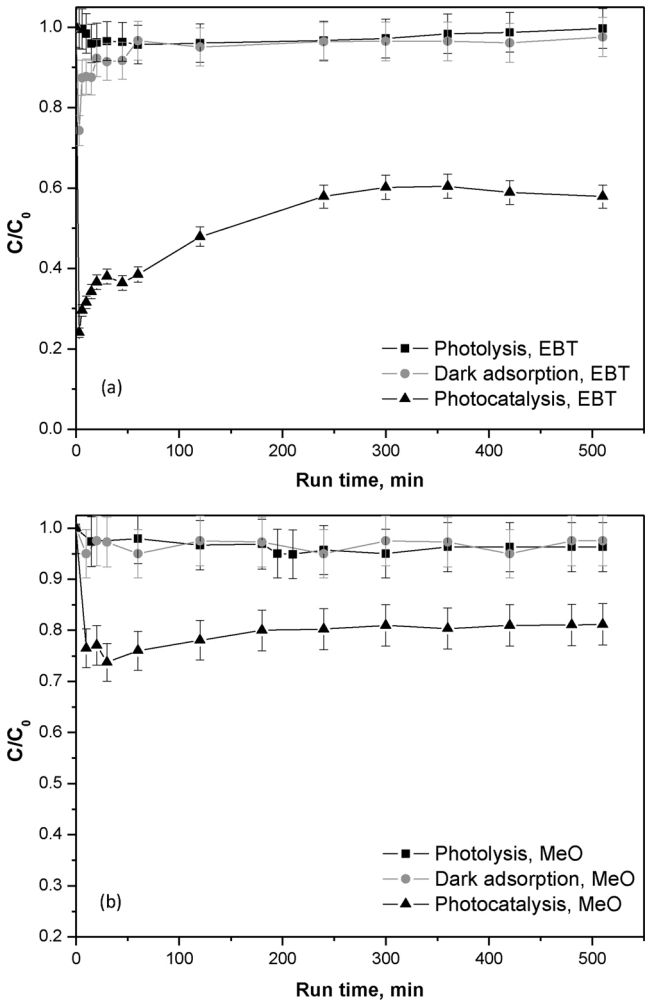

Fig. 4. Photolysis, adsorption and adsorption/photocatalysis tests in the presence of a) EBT and b) MeO in the packed-bed reactor operating in continuous mode; EBT and MeO initial concentration: 10 mg/L; T_PTs catalyst amount: 4 g; Liquid flow rate : 2.1 mL/min.

Different results were reported by Suhadolnik et al. [73], showing that only 10 % of dye degradation was obtained in their continuous system. This efficiency was further improved to 100 % using a more sophisticated design that utilizes a complicated hybrid system of photo-electro catalytic degradation. On the other hand, complete dyes degradation was found using TiO_2 on glass plates [48]. In comparison to the latter, our study achieved similar photocatalytic degradation performances using an efficient and simple design based on the use of commercial TiO_2 sample.

3.3.2. Influence of the liquid flow rate on photocatalytic performances

The influence of EBT and MeO aqueous solution flow rate was studied in terms of the decolourization of the two target dyes (Fig. 5).

The chosen flow rate has been varied in the range from 0.5 to 2.1 mL/min. The results concerning the EBT decolourization are reported in Fig. 5a. With the increase of contact time, the decolourization of EBT increased, leading to an improvement in the performances of the system. In details, using a flow rate equal to 2.1 mL/min, which corresponds to a contact time of 0.7 min, it is possible to observe that, in the first 180 min of the test, the kinetics of adsorption phenomena was higher than the photocatalytic one [41], while after about 380 min and until the end of the test (510 min), the EBT decolourization value became stationary, reaching a decolourization value equal to 39 %. In the same manner, with a liquid flow rate of 0.9 mL/min (contact time of 1.6 min), the trend of the curve is very similar to the previous case, obtaining, after 300 min, 61 % decolourization of EBT dye. The best results in terms of EBT decolourization was achieved with a flow rate of 0.5 mL/min (contact time equal to 3.3 min); in fact, already after 85 min of run time, the steady-state concentration value was reached with 80 % of EBT decolourization. It is important to underline that, also in this case, the decolourization value remained constant for the entire duration of the test (510 min). This means that the T_PTs photocatalyst together with UV light is able to continuously regenerate the active sites of the T_PTs sample, as earlier observed in our previous work dealing with the removal of crystal violet dye by means of a continuous photoreactor [41]. Similar results were achieved for MeO decolouration (Fig. 5b). In particular, with the decrease of the liquid flow rate, there was an improvement of the performances of the T_PTs photocatalyst in the presence of UV light. The best result, also in this case, was obtained with a flow rate equal to 0.5 mL/min. In this operating condition, the MeO decolourization was equal to 54 % for the overall test time.

3.3.3. Influence of the water matrix on T_PTs photocatalyst

For the scale-up of photocatalytic water treatment process, it is

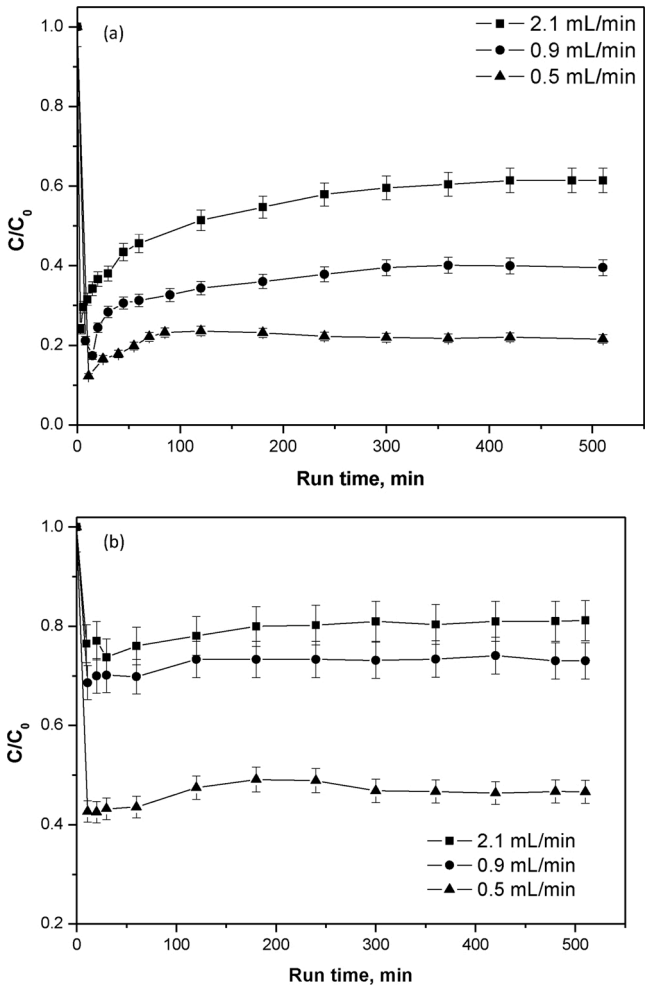

Fig. 5. Adsorption/photocatalysis tests in the presence of a) EBT and b) MeO in the packed-bed reactor operating in continuous mode at different liquid flow rate (0.5–2.1 mL/min); EBT and MeO initial concentration: 10 mg/L; T_PTs catalyst amount: 4 g.

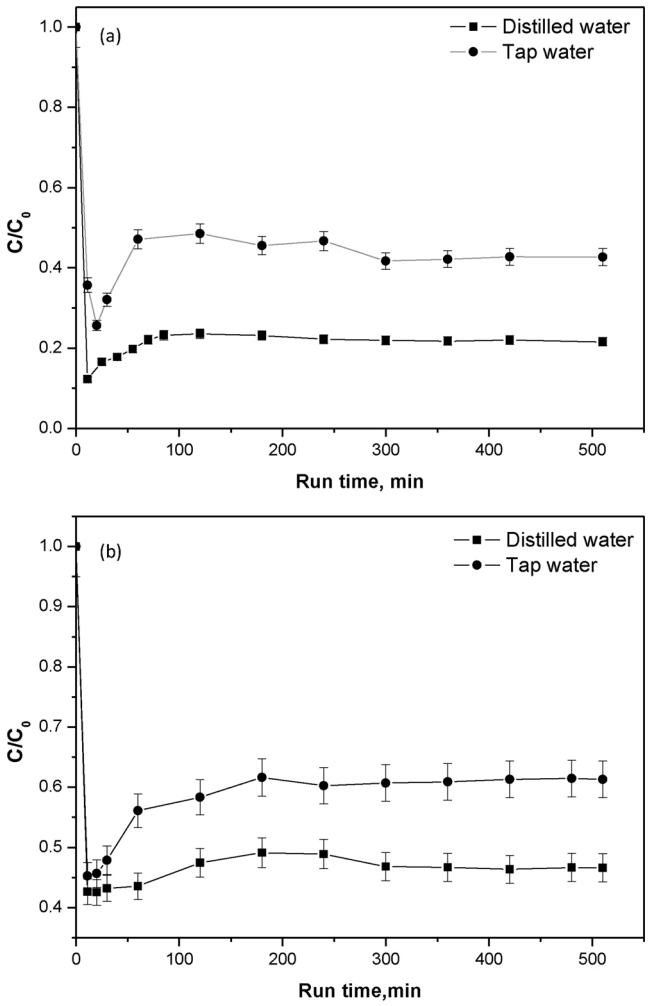

Fig. 6. Comparison of adsorption/photocatalysis tests in the presence of a) EBT and b) MeO in the packed-bed reactor operating in continuous mode using different water matrix (distilled water or tap water); EBT and MeO initial concentration: 10 mg/L; T_PTs catalyst amount: 4 g; liquid flow rate: 0.5 mL/min.

important to evaluate the influence of various inorganic ions commonly present in real water matrix on decolourization rate of the selected organic dyes. In particular, in the literature, it is reported that the presence of inorganic anions such as nitrate, chlorides, carbonates and sulphates generally inhibit the activity of photocatalysts leading to a decreased efficiency in pollutant photodegradation [74]. Moreover, generally, inorganic ions can induce fouling phenomena of the TiO_2 surface, scavenging both the hole and the hydroxyl radicals [75]. Fig. 6 evidences that the presence of inorganic ions contained in the used tap water (Table 1) led to a lower EBT decolourization. The EBT decolourization reached a steady-state value of about 58 % after 300 min of process time and, therefore, a lower value than that one achieved in the presence of distilled water (80 %) (Fig. 6a).

A similar effect was observed for MeO dye (Fig. 6b). The dye decolourization reached a steady-state value of about 40 % after 180 min, lower than those one observed in the presence of distilled water (54 %). In order to enhance the decolourization efficiency of the target dye, the contact time was further increased from 3.3 up to 6.6 min by using a system consisting of two packed-bed reactors of equal geometry in series filled with 4 g of T_PTs each.

Fig. 7 shows the experimental results both with tap and distilled water, evidencing that in the case of EBT decolourization, the photocatalytic system was able to assure the total dye decolourization (Fig. 7a). From the results reported in Fig. 7b, it is evident that the use of two photocatalytic reactors allowed to increase also the MeO decolourization efficiency with respect to the single reactor (Fig. 6b). In detail, despite the MeO molecules were not adsorbed on the T_PTs surface, during the entire test time, the presence of a greater quantity of photocatalyst (T_PTs) irradiated by LED-UV, allowed to obtain a removal of the pollutant equal to 90 % using distilled water and 70 % using tap water, evidencing that, despite the increase in efficiency, the use of two reactors in series, did not assure the total MeO decolourization. For this reason, a hybrid process has been developed for the treatment of the tap water spiked with MeO (at 10 mg/L initial concentration). In detail, the photocatalytic unit was followed by adsorption unit. The two units operated in continuous mode using a liquid flow rate equal to 0.5 mL/min. The photocatalytic unit (consisting of the two photoreacotrs in series) was overall filled with 8 g of T_PTs while the adsorption unit was filled with 4 g of PaC. In this way, at the outlet of the photocatalytic unit, MeO decolourization efficiency was equal to 70 % and increased up to almost 100 % at the outlet of the adsorption unit (Fig. 8). In summary, the experimental results reported in Fig. 8 showed that thanks to the photocatalytic unit followed by an adsorption process, the total MeO decolourization was achieved at the outlet of the overall system.

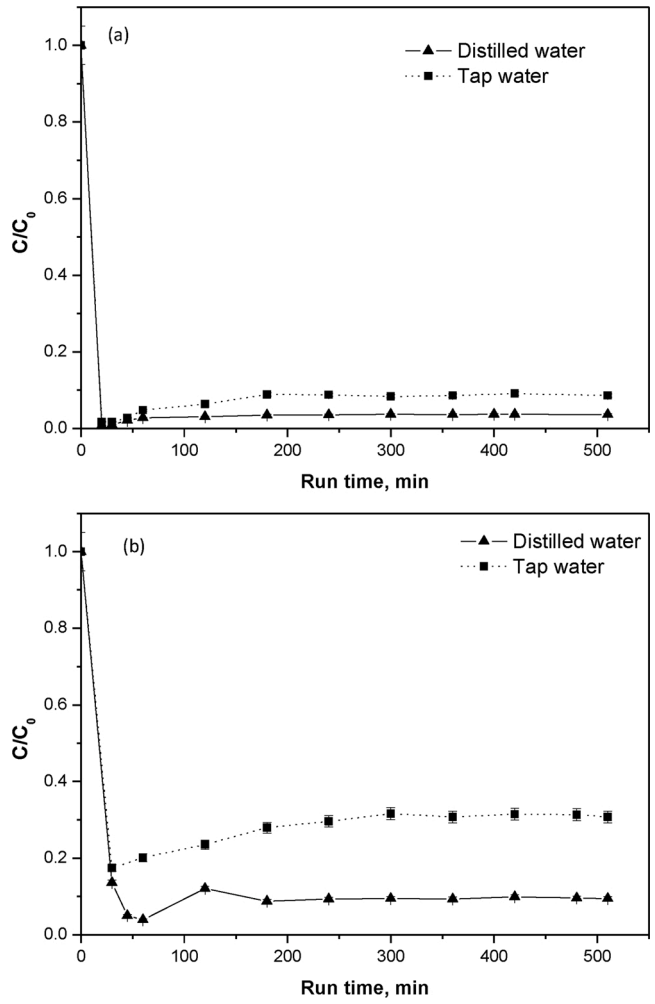

Fig. 7. Adsorption/photocatalysis test in the presence of a) EBT and b) MeO using two continuous flow packed-bed reactors in series with different water matrix (distilled water or tap water); EBT and MeO initial concentration: 10 mg/L; T_PTs catalyst amount: 8 g; liquid flow rate: 0.5 mL/min.

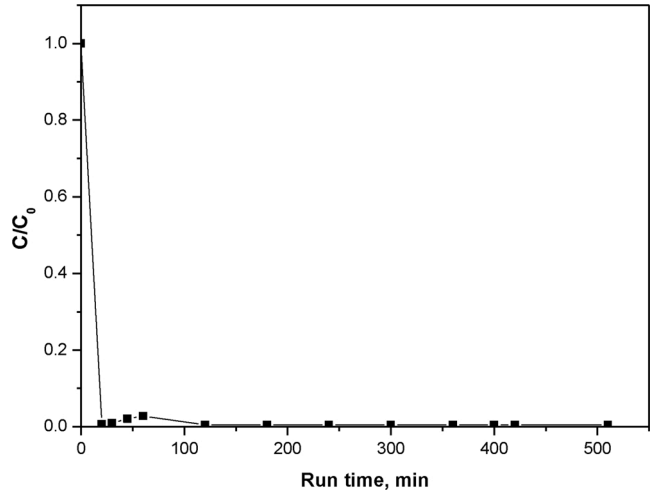

Fig. 8. Behavior of MeO relative concentration in the tap water at the outlet of the photocatalytic unit (composed by two packed-bed reactor in series) followed by adsorption unit filled with pelletized activated carbon; T_PTs catalyst amount: 8 g; PaC amount: 4 g; liquid flow rate:0.5 mL/min.

3.4. Ecotoxicity

Although dyes pose a potential environmental risk, the literature offers only limited information about their ecotoxicity [2,13,15,16]. Croce et al. [2] reported that according to their survey carried out in 2016 on ECHA registered dyes, only 100 monoconstituent organic substances are registered and only a limited number of these dyes (16 %) are characterized by data about aquatic toxicity to *daphnia* and algae suitable for REACH. Ecotoxicity data were provided in Fig. S1 (one packed-bed reactor) and S2 (two packed-bed reactors) in Supplementary Materials (SM) for both MeO and EBT for all the considered exposure scenarios including distilled and tap water and all testing species. Data were normally distributed and homoscedastic. In SMs, the results from each scenario were presented and discussed in detail evidencing that *D. magna* and *R. subcapitata* were the most sensitive testing organisms for both dyes [2]. In order to provide a final and integrated assessment of the results, data were presented in Table 3 according to the class weight score approach [60]. Results evidenced that toxicity was never up to score 1 (slight acute hazard) both in treated and untreated samples. The treatment with one packed-bed reactor showed limited effects in toxicity removal from treated specimen for both MeO and EBT, evidencing in the case of "MeO tap water 0.5 mL/min" condition a toxicity increase compared to the control probably due to the generation of more toxic by-products, similarly to "EBT distilled water 0.9 and 2.1 mL/min" scenarios. The use of two reactors in series did not change the results for EBT "tap water" scenario compared to the treatment with one reactor, similarly to MeO. In the case of MeO, the full toxicity removal was obtained only after PAC filtration. Thus, the total removal of toxicity for EBT can be achieved with just one packed-bed reactor being the toxicity of potential by-products not relevant. Toxicity data are in line with MeO and EBT degradation kinetics.

4. Conclusions

A continuous flow photocatalytic packed-bed reactor irradiated by UV-LEDs was used for the degradation of two anionic azo dyes using commercial TiO_2 pellets (T_PTs) in cylindrical shape (size: 12.5 mm × 5.5 mm). X-ray diffraction analysis and Raman spectroscopy showed that the TiO_2 pellets were in anatase phase. N_2 adsorption-desorption analysis at −196 °C evidenced that T_PTs exhibits pores with mean size of about 6 nm. Moreover, the photocatalyst showed both micro-surface area (10 m^2/g) and meso-surface area (95 m^2/g), underlining that it was mainly composed by mesoporous structure. Eriochrome Black-T (EBT) and Methyl Orange (MeO) were selected as model azo dyes for photocatalytic tests and toxicity assessment. Photocatalytic tests were carried out spiking EBT and MeO both in distilled and tap water. Photocatalytic results showed that, under UV light, the continuous packed-bed reactor allowed to achieve steady-state conditions

Table 3
Integrated class weight score considering each treatment scenario; 0 = no acute hazard; 1 = slight acute hazard; * = untreated spiked solution (10 mg/L); ranking according to [60].

Treatment scenario			MeO	EBT
1 packed-bed reactor	distilled water	Control*	1	0
		0.5 mL/min	1	0
		0.9 mL/min	1	1
		2.1 mL/min	1	1
	tap water	Control*	0	0
		0.5 mL/min	1	0
2 packed-bed reactors	distilled water	Control*	1	0
		0.5 mL/min	1	1
	tap water	Control*	0	0
		0.5 mL/min	1	0
	tap water	control	0	
		PAC	1	
		0.5 mL/min + PAC	0	

without evidencing deactivation phenomena. In the case of distilled water as aqueous matrix, the highest decolourization efficiency (EBT and MeO decolorization of about 100 % and 90 %, respectively) was achieved using a liquid flow rate of 0.5 mL/min, corresponding to a contact time equal to 6.6 min. Using the optimized contact time, in presence of tap water spiked with the dyes, the max % of EBT decolourization and the total removal of toxicity were achieved, whereas MeO degradation was lower (about 70 %). To increase the MeO decolourization performance in presence of tap water, the photocatalytic system was coupled to a subsequent adsorption unit filled with commercial activated carbon reaching the almost total MeO decolourization as well as toxicity removal.

CRediT authorship contribution statement

Vincenzo Vaiano: Validation, Investigation, Writing - original draft, Writing - review & editing. **Olga Sacco:** Conceptualization, Supervision, Investigation, Writing - review & editing, Writing - original draft. **Giovanni Libralato:** Validation, Investigation, Writing - original draft, Writing - review & editing. **Giusy Lofrano:** Validation, Investigation, Writing - review & editing, Writing - original draft. **Antonietta Siciliano:** Investigation, Methodology, Formal analysis, Writing - review & editing. **Federica Carraturo:** Investigation, Methodology, Formal analysis, Writing - review & editing. **Marco Guida:** Investigation, Methodology, Formal analysis, Writing - review & editing. **Maurizio Carotenuto:** Investigation, Methodology, Formal analysis, Writing - review & editing.

Declaration of Competing Interest

The authors report no declarations of interest.

Acknowledgments

A special thank is given to Dott. Emma Iannone for the support given in the photocatalytic tests.

Appendix A. Supplementary data

Supplementary material related to this article can be found, in the online version, at doi:https://doi.org/10.1016/j.jece.2020.104549.

References

[1] G. Lofrano, G. Libralato, M. Carotenuto, M. Guida, M. Inglese, A. Siciliano, S. Meriç, Emerging concern from short-term textile leaching: a preliminary ecotoxicological survey, Bull. Environ. Contam. Toxicol. 97 (2016) 646–652.
[2] R. Croce, F. Cinà, A. Lombardo, G. Crispeyn, C.I. Cappelli, M. Vian, S. Maiorana, E. Benfenati, D. Baderna, Aquatic toxicity of several textile dye formulations: acute and chronic assays with Daphnia magna and Raphidocelis subcapitata, Ecotoxicol. Environ. Saf. 144 (2017) 79–87.
[3] A. Tkaczyk, K. Mitrowska, A. Posyniak, Synthetic organic dyes as contaminants of the aquatic environment and their implications for ecosystems: a review, Sci. Total Environ. (2020), 137222.
[4] A. Bafana, S.S. Devi, T. Chakrabarti, Azo dyes: past, present and the future, Environ. Rev. 19 (2011) 350–371.
[5] R. Ahmad, R. Kumar, Adsorptive removal of congo red dye from aqueous solution using bael shell carbon, Appl. Surf. Sci. 257 (2010) 1628–1633.
[6] A. Khan, X. Wang, K. Gul, F. Khuda, Z. Aly, A. Elseman, Microwave-assisted spent black tea leaves as cost-effective and powerful green adsorbent for the efficient removal of Eriochrome black T from aqueous solutions, Egypt. J. Basic Appl. Sci. 5 (2018) 171–182.
[7] K.-W. Jung, B.H. Choi, S.Y. Lee, K.-H. Ahn, Y.J. Lee, Green synthesis of aluminum-based metal organic framework for the removal of azo dye Acid Black 1 from aqueous media, J. Ind. Eng. Chem. 67 (2018) 316–325.
[8] A. Pirkarami, M.E. Olya, F. Najafi, Removal of azo dye from aqueous solution using an anionic polymeric urethane absorbent (APUA), J. Ind. Eng. Chem. 21 (2015) 387–393.
[9] J.B. Parsa, M. Golmirzaei, M. Abbasi, Degradation of azo dye C.I. Acid Red 18 in aqueous solution by ozone-electrolysis process, J. Ind. Eng. Chem. 20 (2014) 689–694.
[10] Y. Jin, N. Li, H. Liu, X. Hua, Q. Zhang, M. Chen, F. Teng, Highly efficient degradation of dye pollutants by Ce-doped MoO 3 catalyst at room temperature, J. Chem. Soc. Dalton Trans. 43 (2014) 12860–12870.
[11] R.P. Singh, P.K. Singh, R.L. Singh, Bacterial decolorization of textile azo dye acid orange by Staphylococcus hominis RMLRT03, Toxicol. Int. 21 (2014) 160.
[12] P.K. Arora, Bacterial degradation of monocyclic aromatic amines, Front. Microbiol. 6 (2015) 820.
[13] C. Wang, A. Yediler, D. Lienert, Z. Wang, A. Kettrup, Toxicity evaluation of reactive dyestuffs, auxiliaries and selected effluents in textile finishing industry to luminescent bacteria Vibrio fischeri, Chemosphere 46 (2002) 339–344.
[14] S. Srivastava, R. Sinha, D. Roy, Toxicological effects of malachite green, Aquat. Toxicol. 66 (2004) 319–329.
[15] V. Suryavathi, S. Sharma, S. Sharma, P. Saxena, S. Pandey, R. Grover, S. Kumar, K. Sharma, Acute toxicity of textile dye wastewaters (untreated and treated) of Sanganer on male reproductive systems of albino rats and mice, Reprod. Toxicol. 19 (2005) 547–556.
[16] J.-S. Bae, H.S. Freeman, Aquatic toxicity evaluation of new direct dyes to the Daphnia magna, Dye. Pigment. 73 (2007) 81–85.
[17] G. Dave, P. Aspegren, Comparative toxicity of leachates from 52 textiles to Daphnia magna, Ecotoxicol. Environ. Saf. 73 (2010) 1629–1632.
[18] T. Rasheed, F. Nabeel, M. Bilal, H.M. Iqbal, Biogenic synthesis and characterization of cobalt oxide nanoparticles for catalytic reduction of direct yellow-142 and methyl orange dyes, Biocatal. Agric. Biotechnol. 19 (2019), 101154.
[19] M.S. Manzar, A. Waheed, I.W. Qazi, N.I. Blaisi, N. Ullah, Synthesis of a novel epibromohydrin modified crosslinked polyamine resin for highly efficient removal of methyl orange and eriochrome black T, J. Taiwan Inst. Chem. Eng. 97 (2019) 424–432.
[20] N. Barka, M. Abdennouri, M.E. Makhfouk, Removal of Methylene Blue and Eriochrome Black T from aqueous solutions by biosorption on Scolymus hispanicus L.: kinetics, equilibrium and thermodynamics, J. Taiwan Inst. Chem. Eng. 42 (2011) 320–326.
[21] J.-H. Park, J.J. Wang, N. Tafti, R.D. Delaune, Removal of Eriochrome Black T by sulfate radical generated from Fe-impregnated biochar/persulfate in Fenton-like reaction, J. Ind. Eng. Chem. 71 (2019) 201–209.
[22] M. Arshadi, A. Faraji, M. Amiri, M. Mehravar, A. Gil, Removal of methyl orange on modified ostrich bone waste–A novel organic–inorganic biocomposite, J. Colloid Interface Sci. 446 (2015) 11–23.
[23] O.A. Attallah, M.A. Al-Ghobashy, M. Nebsen, M.Y. Salem, Removal of cationic and anionic dyes from aqueous solution with magnetite/pectin and magnetite/silica/pectin hybrid nanocomposites: kinetic, isotherm and mechanism analysis, RSC Adv. 6 (2016) 11461–11480.
[24] M.D.G. de Luna, E.D. Flores, D.A.D. Genuino, C.M. Futalan, M.-W. Wan, Adsorption of Eriochrome Black T (EBT) dye using activated carbon prepared from waste rice hulls—optimization, isotherm and kinetic studies, J. Taiwan Inst. Chem. Eng. 44 (2013) 646–653.
[25] Y. Yasin, A.H. Abdul Malek, S. Mariam Sumari, Adsorption of eriochrome black dye from aqueous solution onto anionic layered double hydroxides, Orient. J. Chem. 26 (2010) 1293.
[26] F. Moeinpour, A. Alimoradi, M. Kazemi, Efficient removal of Eriochrome black-T from aqueous solution using NiFe 2 O 4 magnetic nanoparticles, J. Environ. Health Sci. Eng. 12 (2014) 112.
[27] J. Liu, J.C. Crittenden, D.W. Hand, D.L. Perram, Regeneration of adsorbents using heterogeneous photocatalytic oxidation, J. Environ. Eng. 122 (1996) 707–713.
[28] S. Lee, J.-S. Lee, M.-K. Song, J.-C. Ryu, B. An, C.-G. Lee, C. Park, S.-H. Lee, J.-W. Choi, Effective regeneration of an adsorbent for the removal of organic contaminants developed based on UV radiation and toxicity evaluation, React. Funct. Polym. 95 (2015) 62–70.
[29] K. Paixão, E. Abreu, G.R.L. Samanamud, A.B. França, C.C.A. Loures, E.P. Baston, L. L.R. Naves, J.C. Bosch, F.L. Naves, Normal boundary intersection applied in the scale-up for the treatment process of Eriochrome Black T through the UV/TiO2/O3 system, J. Environ. Chem. Eng. 7 (2019), 102801.
[30] G. Vilardi, J.M. Ochando-Pulido, M. Stoller, N. Verdone, L. Di Palma, Fenton oxidation and chromium recovery from tannery wastewater by means of iron-based coated biomass as heterogeneous catalyst in fixed-bed columns, Chem. Eng. J. 351 (2018) 1–11.
[31] S. Mozia, A.W. Morawski, M. Toyoda, M. Inagaki, Application of anatase-phase TiO2 for decomposition of azo dye in a photocatalytic membrane reactor, Desalination 241 (2009) 97–105.
[32] M.R. Hoffmann, S.T. Martin, W. Choi, D.W. Bahnemann, Environmental applications of semiconductor photocatalysis, Chem. Rev. 95 (1995) 69–96.
[33] V. Vaiano, O. Sacco, D. Sannino, M. Stoller, P. Ciambelli, A. Chianese, Photocatalytic removal of phenol by ferromagnetic N-TiO2/SiO2/Fe3O4 nanoparticles in presence of visible light irradiation, Chem. Eng. Trans. 47 (2016) 235–240.
[34] V. Vaiano, G. Sarno, O. Sacco, D. Sannino, Degradation of terephthalic acid in a photocatalytic system able to work also at high pressure, Chem. Eng. J. 312 (2017) 10–19.
[35] F. Parrino, V. Loddo, V. Augugliaro, G. Camera-Roda, G. Palmisano, L. Palmisano, S. Yurdakal, Heterogeneous photocatalysis: guidelines on experimental setup, catalyst characterization, interpretation, and assessment of reactivity, Catal. Rev. - Sci. Eng. 61 (2019) 163–213.
[36] Y. Chen, D.D. Dionysiou, TiO2 photocatalytic films on stainless steel: the role of Degussa P-25 in modified sol–gel methods, Appl. Catal. B 62 (2006) 255–264.
[37] G. Maniakova, K. Kowalska, S. Murgolo, G. Mascolo, G. Libralato, G. Lofrano, O. Sacco, M. Guida, L. Rizzo, Comparison between heterogeneous and

homogeneous solar driven advanced oxidation processes for urban wastewater treatment: pharmaceuticals removal and toxicity, Sep. Purif. Technol. 236 (2020).
[38] K. Kowalska, G. Maniakova, M. Carotenuto, O. Sacco, V. Vaiano, G. Lofrano, L. Rizzo, Removal of carbamazepine, diclofenac and trimethoprim by solar driven advanced oxidation processes in a compound triangular collector based reactor: a comparison between homogeneous and heterogeneous processes, Chemosphere 238 (2020).
[39] O. Sacco, V. Vaiano, C. Daniel, W. Navarra, V. Venditto, Highly robust and selective system for water pollutants removal: how to transform a traditional photocatalyst into a highly robust and selective system for water pollutants removal, Nanomaterials 9 (2019).
[40] O. Sacco, V. Vaiano, C. Daniel, W. Navarra, V. Venditto, Removal of phenol in aqueous media by N-doped TiO2 based photocatalytic aerogels, Mater. Sci. Semicond. Process. 80 (2018) 104–110.
[41] O. Sacco, M. Matarangolo, V. Vaiano, G. Libralato, M. Guida, G. Lofrano, M. Carotenuto, Crystal violet and toxicity removal by adsorption and simultaneous photocatalysis in a continuous flow micro-reactor, Sci. Total Environ. 644 (2018) 430–438.
[42] S. Malato, J. Blanco, A. Vidal, C. Richter, Photocatalysis with solar energy at a pilot-plant scale: an overview, Appl. Catal. B: Environ. 37 (2002) 1–15.
[43] Y.-c. Li, L.-d. Zou, E. Hu, Photocatalytic degradation of dye effluent by titanium dioxide pillar pellets in aqueous solution, J. Environ. Sci. 16 (2004) 375–379.
[44] A. Akyol, M. Bayramoglu, The degradation of an azo dye in a batch slurry photocatalytic reactor, Chem. Eng. Process. Process. Intensif. 47 (2008) 2150–2156.
[45] M.E. Olya, A. Pirkarami, Cost-effective photoelectrocatalytic treatment of dyes in a batch reactor equipped with solar cells, Sep. Purif. Technol. 118 (2013) 557–566.
[46] H. Lachheb, E. Puzenat, A. Houas, M. Ksibi, E. Elaloui, C. Guillard, J.-M. Herrmann, Photocatalytic degradation of various types of dyes (Alizarin S, Crocein Orange G, Methyl Red, Congo Red, Methylene Blue) in water by UV-irradiated titania, Appl. Catal. B 39 (2002) 75–90.
[47] K. Tanaka, K. Padermpole, T. Hisanaga, Photocatalytic degradation of commercial azo dyes, Water Res. 34 (2000) 327–333.
[48] M. Behnajady, N. Modirshahla, N. Daneshvar, M. Rabbani, Photocatalytic degradation of an azo dye in a tubular continuous-flow photoreactor with immobilized TiO2 on glass plates, Chem. Eng. J. 127 (2007) 167–176.
[49] J. Chanathaworn, J. Pornpunyapat, J. Chungsiriporn, Decolorization of dyeing wastewater in continuous photoreactors using tio 2 coated glass tube media, Songklanakarin J. Sci. Technol. 36 (2014).
[50] V. Vaiano, O. Sacco, D. Pisano, D. Sannino, P. Ciambelli, From the design to the development of a continuous fixed bed photoreactor for photocatalytic degradation of organic pollutants in wastewater, Chem. Eng. Sci. 137 (2015) 152–160.
[51] S.K. Kansal, S. Sood, A. Umar, S. Mehta, Photocatalytic degradation of Eriochrome Black T dye using well-crystalline anatase TiO2 nanoparticles, J. Alloys. Compd. 581 (2013) 392–397.
[52] R. Cai, B. Zhang, J. Shi, M. Li, Z. He, Rapid photocatalytic decolorization of methyl orange under visible light using VS4/carbon powder nanocomposites, ACS Sustain. Chem. Eng. 5 (2017) 7690–7699.
[53] G. Lofrano, G. Libralato, R. Adinolfi, A. Siciliano, P. Iannece, M. Guida, M. Giugni, A.V. Ghirardini, M. Carotenuto, Photocatalytic degradation of the antibiotic chloramphenicol and effluent toxicity effects, Ecotoxicol. Environ. Saf. 123 (2016) 65–71.
[54] G. Lofrano, G. Libralato, A. Casaburi, A. Siciliano, P. Iannece, M. Guida, L. Pucci, E. Dentice, M. Carotenuto, Municipal wastewater spiramycin removal by conventional treatments and heterogeneous photocatalysis, Sci. Total Environ. 624 (2018) 461–469.
[55] E. ISO, Water Quality—Determination of the Inhibition of the Mobility of Daphnia magna Straus (Cladocera, Crustacea)—Acute toxicity Test, EN ISO, 1998, p. 1996, 6341.
[56] E. ISO, 8692, Water Quality—freshwater Algal Growth Inhibition Test With Unicellular Green Algae, European Committee for Standardization, Brusel, 2012 (2012).
[57] M. Richard, Development Co-Operation Report 2007, OECD Publishing, 2008.
[58] M. Beltrami, D. Rossi, R. Baudo, Phytotoxicity assessment of Lake Orta sediments, Aquat. Ecosyst. Health Manage. 2 (1999) 391–401.
[59] G. Libralato, A.C. Devoti, M. Zanella, E. Sabbioni, I. Mičetić, L. Manodori, A. Pigozzo, S. Manenti, F. Groppi, A.V. Ghirardini, Phytotoxicity of ionic, micro- and nano-sized iron in three plant species, Ecotoxicol. Environ. Saf. 123 (2016) 81–88.
[60] G. Persoone, B. Marsalek, I. Blinova, A. Törökne, D. Zarina, L. Manusadzianas, G. Nalecz-Jawecki, L. Tofan, N. Stepanova, L. Tothova, A practical and user-friendly toxicity classification system with microbiotests for natural waters and wastewaters, Environ. Toxicol.: Int. J. 18 (2003) 395–402.
[61] G. Libralato, V.G. Annamaria, A. Francesco, How toxic is toxic? A proposal for wastewater toxicity hazard assessment, Ecotoxicol. Environ. Saf. 73 (2010) 1602–1611.
[62] P.S. Dunlop, A. Galdi, T.A. McMurray, J.W. Hamilton, L. Rizzo, J.A. Byrne, Comparison of photocatalytic activities of commercial titanium dioxide powders immobilised on glass substrates, J. Adv. Oxid. Technol. 13 (2010) 99–106.
[63] L. Rizzo, D. Sannino, V. Vaiano, O. Sacco, A. Scarpa, D. Pietrogiacomi, Effect of solar simulated N-doped TiO2 photocatalysis on the inactivation and antibiotic resistance of an E. coli strain in biologically treated urban wastewater, Appl. Catal. B: Environ. 144 (2014) 369–378.
[64] L. Stagi, C.M. Carbonaro, R. Corpino, D. Chiriu, P.C. Ricci, Light induced TiO2 phase transformation: correlation with luminescent surface defects, Phys. Status Solidi B 252 (2015) 124–129.
[65] L. Alemany, M. Bañares, E. Pardo, F. Martın-Jiménez, J. Blasco, Morphological and structural characterization of a titanium dioxide system, Mater. Charact. 44 (2000) 271–275.
[66] C.L. Bianchi, C. Pirola, M. Stucchi, B. Sacchi, G. Cerrato, S. Morandi, A. Di Michele, A. Carletti, V. Capucci, A New Frontier of Photocatalysis Employing Micro-Sized TiO2: Air/Water Pollution Abatement and Self-Cleaning/Antibacterial Applications, 2016.
[67] M. Thommes, K. Kaneko, A.V. Neimark, J.P. Olivier, F. Rodriguez-Reinoso, J. Rouquerol, K.S. Sing, Physisorption of gases, with special reference to the evaluation of surface area and pore size distribution (IUPAC Technical Report), Pure Appl. Chem. 87 (2015) 1051–1069.
[68] V. Vaiano, M. Matarangolo, O. Sacco, D. Sannino, Photocatalytic removal of eriochrome black T dye over ZnO nanoparticles doped with Pr, Ce or Eu, Chem. Eng. Trans. 57 (2017) 625–630.
[69] T. Kodom, E. Amouzou, G. Djaneye-Boundjou, L.M. Bawa, P. Acevedo-Pena, G. Vazquez, D. Laverde, J. Pedraza-Rosas, J. Manriquez, I. Gonzalez, The preparation and chemical structure of TiO2 film photocatalysts supported on stainless steel substrates via the sol-gel method, Int. J. Chem. Technol. 4 (2009) C377–C386.
[70] A.F. Halbus, F.H. Hussein, Heterogeneous photocatalytic decolourization of cobalamine in the presence of aqueous titanium dioxide suspensions, Asian J. Chem. 24 (2012) 5579.
[71] M. Bootharaju, T. Pradeep, Facile and rapid synthesis of a dithiol-protected Ag7 quantum cluster for selective adsorption of cationic dyes, Langmuir 29 (2013) 8125–8132.
[72] E. Colombo, M. Ashokkumar, Comparison of the photocatalytic efficiencies of continuous stirred tank reactor (CSTR) and batch systems using a dispersed micron sized photocatalyst, RSC Adv. 7 (2017) 48222–48229.
[73] L. Suhadolnik, A. Pohar, U. Novak, B. Likozar, A. Mihelič, M. Čeh, Continuous photocatalytic, electrocatalytic and photo-electrocatalytic degradation of a reactive textile dye for wastewater-treatment processes: batch, microreactor and scaled-up operation, J. Ind. Eng. Chem. 72 (2019) 178–188.
[74] J. Colmenares, M. Aramendia, A. Marinas, J. Marinas, F. Urbano, Synthesis, characterization and photocatalytic activity of different metal-doped titania systems, Appl. Catal. A Gen. 306 (2006) 120–127.
[75] A. Kumar, G. Pandey, A review on the factors affecting the photocatalytic degradation of hazardous materials, Adv. Mater. Sci. Eng. Int. J. 1 (2017) 1–10.